# *CHD1L* is associated with poor survival and promotes the proliferation and metastasis of intrahepatic cholangiocarcinoma

SHIMIAO LI[1*], YI CHAI[2,3*], YANBAO DING[4], TINGHAO YUAN[4], CHANGWEN WU[5] and CHANGWEN HUANG[1]

[1]Department of Hepatobiliary Surgery, Jiangxi Provincial People's Hospital, Nanchang, Jiangxi 330006; [2]Department of Neurosurgery, Yuquan Hospital, School of Clinical Medicine, Tsinghua University, Beijing 100040; [3]Department of Neurosurgery, Shangrao People's Hospital, Shangrao, Jiangxi 334000; Departments of [4]Hepatobiliary Surgery and [5]Urology Surgery, The Second Affiliated Hospital of Nanchang University, Nanchang, Jiangxi 330006, P.R. China

Received November 19, 2018; Accepted May 17, 2019

DOI: 10.3892/or.2019.7174

**Abstract.** Chromodomain helicase/ATPase DNA-binding protein 1-like gene (*CHD1L*) is a new oncogene which has been confirmed to be crucial to the progression of many solid tumors. In the present study, the expression of *CHD1L* was found to be upregulated in intrahepatic cholangiocarcinoma (ICC), which was significantly associated with histological differentiation (P=0.011), vascular invasion (P=0.002), lymph node metastasis (P=0.008) and TNM stage (P=0.001). Kaplan-Meier survival analysis revealed that ICC patients with positive *CHD1L* expression had shorter overall and disease-free survival than those with negative *CHD1L* expression. Functional study found that *CHD1L* exhibited strong oncogenic roles, including increased cell growth by CCK-8 assay, colony formation by plate colony formation assay, G1/S transition by flow cytometry and tumor formation in nude mice. In addition, RNAi-mediated silencing of *CHD1L* inhibited ICC invasion and metastasis by wound healing, Transwell migration and Matrigel invasion assays *in vitro* and *in vivo*. Collectively, our results show that *CHD1L* is upregulated and promotes the proliferation and metastasis of ICC cells. *CHD1L* acts as an oncogene and may be a prognostic factor or therapeutic target for patients with ICC.

*Correspondence to:* Dr Changwen Huang, Department of Hepatobiliary Surgery, Jiangxi Provincial People's Hospital, 92 Aiguo Road, Nanchang, Jiangxi 330006, P.R. China
E-mail: ncdxhcw@163.com

*Contributed equally

*Abbreviations: CHD1L*, chromodomain helicase/ATPase DNA-binding protein 1-like gene; ICC, intrahepatic cholangiocarcinoma; HCC, hepatocellular carcinoma; *SNF2*, sucrose non-fermenting 2; EMT, epithelial-mesenchymal transition; MET, mesenchymal-epithelial transition; CTRL, control; LV-shNC, lentivirus-shorthairpin negative control; RT-qPCR, real-time quantitative polymerase chain reaction; IHC, immunohistochemistry; CCK-8, Cell Counting Kit-8; EGFP, enhanced green fluorescent protein; MOCK, empty vector-transfected; HR, hazard ratio; CI, confident interval

*Key words:* intrahepatic cholangiocarcinoma, *CHD1L*, proliferation, metastasis, prognosis

## Introduction

Intrahepatic cholangiocarcinoma (ICC) is the second most common primary hepatobiliary malignancy following hepatocellular carcinoma (1). ICC accounts for approximately 5-10% of all cases of cholangiocarcinoma, and both its incidence and mortality rate have been increasing in recent decades, especially in Southeast Asia (2,3). Despite advances in the diagnosis and treatment of patients with ICC, the prognosis of this disease is still poor, with a 5-year survival of only 25-35% (4). This poor survival rate is due to patients being diagnosed at the advanced stage, when cancer cell invasion into the blood and lymphatic vessels has already led to metastatic spread (5). Therefore, the prognosis of ICC patients may be improved by identifying novel and effective therapeutic targets.

Chromodomain helicase/ATPase DNA-binding protein 1-like gene (*CHD1L*), also named amplified in liver cancer 1 gene (*ALC1*), was first isolated from 1q21 by *Ma et al* (6) in 2008, and it was identified as a target oncogene in hepatocellular carcinoma (HCC) (7). *CHD1L* belongs to the sucrose non-fermenting 2 (*SNF2*)-like subfamily of the *SNF2* family consisting of a helicase superfamily c-terminal (*HELICc*) and a Macro domain (7). Hence, *CHD1L* has also been hypothesized to play important roles in transcriptional regulation, maintenance of chromosome integrity and DNA repair, similar to the *SNF2* family members (7). *CHD1L* was first found to play a vital role in the development and progression of HCC (8). More interestingly, a number of studies have found that amplification of *CHD1L* is extremely common in many solid tumors, including breast (9), gastric (10) and nasopharyngeal carcinoma (11). Recently, He *et al* reported that *CHD1L* protein is overexpressed in human ovarian carcinomas and is a novel predictive biomarker for patient survival (12). However, the expression of *CHD1L* and its significance in ICC is far from clear; even less is known about its function and how *CHD1L* contributes to cancer development and progression.

In the present study, *CHD1L* expression levels were detected in ICC tissues and cell lines. The relationship between *CHD1L*

and clinical characteristics of ICC patients was analyzed, and its oncogene function was examined further *in vitro* and *in vivo*. Our results suggest that *CHD1L* is markedly upregulated and promotes the proliferation and metastasis of ICC cells. *CHD1L* acts as an oncogene and may be a prognostic factor or therapeutic target for patients with ICC.

## Materials and methods

*Patients and tissue samples*. Eighty ICC tissue and thirty hepatolithiasis tissue sections used for paraffin embedding were collected from ICC patients who underwent curative surgery without prior radiotherapy or chemotherapy between January 2007 and January 2012 at the Department of Hepatobiliary Surgery, Jiangxi Provincial People's Hospital (Nanchang, China) and were confirmed by a pathologist. The present study was approved by the Ethics Committee of Jiangxi Provincial People's Hospital, and all patients provided informed consent. The tumor stage was classified according to the 7th tumor-node-metastasis (TNM) classification of the International Union against Cancer (UICC) (13). Among the 80 ICC patients, there were 49 males and 31 females with ages ranging from 42 to 73 years (mean age, 55 years). Information concerning the clinical characteristics and survival prognosis was extracted from medical records and follow-ups. Fresh ICC tissues and paired non-tumor tissue samples were obtained from 34 ICC patients, and these samples were frozen and stored at -80˚C. Paired non-tumor tissues were dissected at least 2 cm away from the cancer border and were verified to lack cancer cells by microscopy.

*RNA extraction and RT-qPCR*. Total RNA was extracted from fresh tissues and cultured cells using TRIzol reagent (TransGen Biotech Co., Ltd., Beijing, China) according to the manufacturer's protocol. cDNA was synthesized from 2 $\mu$g of total RNA using PrimeScript™ RT Master Mix (Takara Bio, Inc., Shiga, Japan). RNA expression was measured by RT-qPCR using the SYBR-Green Fast qPCR Mix in an Applied Biosystems® 7500 Real-Time PCR Systems (Applied Biosystems; Thermo Fisher Scientific, Inc., Waltham, MA, USA) according to the manufacturer's instructions. The $2^{-\Delta\Delta Cq}$ method (14) was used to calculate the expression level (defined as the fold change) of *CHD1L* compared with *GAPDH* expression. Primer sequences are listed in Table I.

*Immunohistochemistry (IHC)*. IHC staining of sections was performed using a standard streptavidin-peroxidase staining method. Paraffin-embedded samples of *CHD1L* expression were cut into 5-$\mu$m-thick sections and processed for IHC method, as previously described by Renshaw (15). Tissue sections with antigen retrieval by microwave treatment in citrate buffer (pH 6.0) were then incubated at 4˚C overnight with primary antibodies for anti-E-cadherin (dilution 1:250; cat. no. sc-71008; Santa Cruz Biotechnology, Santa Cruz, CA, USA), anti-N-cadherin (dilution 1:250; cat. no. sc-53488; Santa Cruz Biotechnology) and anti-*CHD1L* (dilution 1:500; cat. no. ab-197019; Abcam, Cambridge, MA, USA). Immunostaining was performed using Mayer's hematoxylin (Beyotime Biotechnology Institute of Biotechnology, Shanghai, China) and images were captured and assessed using a light microscope (Olympus Corp., Tokyo, Japan). The degree of immunostaining of sections was reviewed and estimated independently by two observers in a blinded manner, based on both the staining intensity and the proportion of positive tumor cells (16). The staining intensity was semi-quantitatively classified as 0 (negative), 1 (weak), 2 (intermediate), or 3 (strong). Additionally, the proportion of positive tumor cells was scored as follows: 0, 0-5%, no positive tumor cells; 1, >5-25%, positive tumor cells; 2, >25-50%, positive tumor cells; and 3, >50%, positive tumor cells. The staining index=the staining intensity x proportion of positive tumor cells; the final immunoreaction score was defined as negative (0-1), weak (2-3), moderate (4-6) and strong (6-9) staining. For statistical purposes, the staining index score was graded as negative (negative and weak) or positive (moderate and strong) expression.

*Cell lines and cell culture*. The human ICC cell lines RBE and HCCC9810 were purchased from the Cell Bank of the Chinese Academy of Sciences (Shanghai, China), and cell lines QBC939 and HuCCT1 were obtained from the American Type Culture Collection (ATCC, Manassas, VA, USA). Human intrahepatic biliary epithelial cells (HiBECs) were stored at the Key Molecular Medical Laboratory of Jiangxi Province (Nanchang, China). Cells were cultured in RPMI-1640 medium (Gibco; Thermo Fisher Scientific, Inc.) supplemented with 10% fetal bovine serum (FBS; Thermo Fisher Scientific, Inc.). Cells were incubated for 48 or 96 h in a humidified incubator supplied with 5% $CO_2$ at 37˚C.

*Antibodies and western blotting*. A rabbit anti-CHD1L antibody was purchased from Abcam (dilution 1:5,000; cat. no. ab197019). Mouse anti-N-cadherin (dilution 1:500; cat. no. sc-53488), anti-E-cadherin (dilution 1:500; cat. no. sc-71008), anti-vimentin (dilution 1:600; cat. no. sc-80975), anti-p53 (dilution 1:600; cat. no. sc-47698), anti-cyclin D1 (dilution 1:750; cat. no. sc-8396) and anti-Cdk2 (dilution 1:750; cat. no. sc-128295; all were from Santa Cruz Biotechnology) antibodies were purchased from Santa Cruz Biotechnology and rabbit anti-GAPDH antibody was obtained from ProteinTech Group, Inc. (Chicago, IL, USA; diluted at 1:10,000). Briefly, equal quantities of cellular proteins were resolved by sodium dodecyl sulfate-polyacrylamide gel electrophoresis, transferred onto polyvinylidene difluoride (PVDF) membranes, and immunoblotted with primary antibodies against CHD1L, N-cadherin, E-cadherin, vimentin, p53, cyclin D1, Cdk2 and GAPDH. After incubation for 1 h at room temperature with horseradish peroxidase (HRP)-conjugated secondary antibody (dilution 1:10,000; cat. no. HS101-01; TransGen Biotech Co., Ltd.), western blot analyses were visualized by enhanced chemiluminescence (EMD Millipore, Billerica, MA, USA). GAPDH was used as the loading control.

*Lentivirus-mediated RNA interference and construction of plasmids*. Silencing of *CHD1L* was carried out using short hairpin RNAs (shRNAs), which were synthesized and inserted into the lentivirus vector containing a cytomegalovirus-driven enhanced green fluorescent protein (EGFP) gene. Vectors expressing *CHD1L*-shRNA (*shCHD1L*) or negative control shRNA (shNC) were designed by Shanghai GeneChem Co., Ltd. (Shanghai, China). The full-length *CHD1L* cDNA was

Table I. Primer sequences of CHD1L and GAPDH.

| Gene promoter | Sequence (5'-3') |
|---|---|
| CHD1L | F: 5'-GGGAAGACCTGCCAGATTTGCT-3' |
| | R: 5'-ACGTGACTCCTGTTTCAGGTCTTG-3' |
| GAPDH | F: 5'-GTTGGAGGTCGGAGTCAACGGA-3' |
| | R: 5'-GAGGGATCTCGCTCCTGGAGGA-3' |

CHD1L, chromodomain helicase/ATPase DNA-binding protein 1-like gene; F, forward; R, reverse.

Table II. Sequences of the CHD1L-RNAi.

| CHD1L-RNAi | Sequence (5'-3') |
|---|---|
| CHD1L-RNAi1 | F: 5'-CGTATTGGACATGCCACGAAA-3' |
| | R:5'-TTTCGTGGCATGTCCAATACG-3' |
| CHD1L-RNAi2 | F: 5'-GCCAAGAGAAGGAGACTCATA-3' |
| | R:5'-TATGAGTCTCCTTCTCTTGGC-3' |
| CHD1L-RNAi3 | F: 5'-GCACAAACTCTTGCAGCCATT-3' |
| | R:5'-AATGGCTGCAAGAGTTTGTGC-3' |
| NC | F: 5'-TTCTCCGAACGTGTCACGT-3' |
| | R:5'-GUGACACGUUCGGAGAAT-3' |

CHD1L, chromodomain helicase/ATPase DNA-binding protein 1-like gene; NC, negative control; F, forward; R, reverse.

cloned into the GV362 expression vector (Shanghai GeneChem Co., Ltd.) and empty vector-transfected cells (MOCK) were used as control. The detailed sequences are listed in Table II. RBE and HUCCT1 cells were transfection with Lv-shRNA in serum-free medium using concentrated virus and replaced with complete culture medium after 24 h. Similarly, the over-expression *CHD1L* and MOCK plasmids were transfected into HCCC9810 cells using Lipofectamine 2000 (Invitrogen; Thermo Fisher Scientific, Inc.). Stably transfected cells were selected for 1-2 weeks by using 500 $\mu$g/ml puromycin (TransGen Biotech Co., Ltd.); *CHD1L* expression in surviving cells was validated by western blotting and RT-qPCR analysis after transfection for 72 h.

*Cell proliferation assay*. Cells after transfection for 24 h were planted at a density of $4x10^4$ cells/well in a 96-well plate and cultured at 37˚C with 5% $CO_2$ in an incubator. Ten microliters of CCK-8 reagent (TransGen Biotech Co., Ltd.) was added to each well at 0, 24, 48, 72 and 96 h and incubated for 2 h. Finally, OD values at 450 nm were measured with a microplate reader, and the growth curve was plotted. Anchorage-independent growth was assessed by a colony formation assay. Briefly, 1,000 cells were seeded in 6-well plates. The cells were cultured for ~1-2 weeks, changed into fresh medium after 2-3 days to see visible clones. Afterwards, cells were fixed with 4% paraformaldehyde for 20 min and stained with 0.1% crystal violet for 30 min. The total number of colonies containing >50 cells and ranging in size from 0.3-1.0 mm was counted, and the images were photographed at x100 magnification under a light microscope.

*Flow cytometry*. ICC cells ($1.5x10^5$ cells) were seeded into 100-mm culture dishes. Twenty-four hours after seeding, the cells were treated with 0.1 or 0.3 mg/ml vehicle (0.1% DMSO) for 24 h. After treatment, the cells at 70-80% confluence were digested into a single-cell suspension, fixed in 70% ethanol, stained with propidium iodide (PI), and analyzed by flow cytometry. In addition, the percentages of cells within each phase of the cell cycle were analyzed with ModFit version 4.0 (Verity Software House, Inc., Topsham, ME, USA) and CellQuest version 5.1 (Thermo Fisher Scientific, Inc.).

*Cell migration and invasion assays*. For the wound healing assay, cells were planted at a density of $5x10^6$ cells/ml in a 6-well plate and incubated at 37˚C overnight. A cell-free area of the culture medium was wounded by scratching with a 200-$\mu$l pipette tip. Cell migration into the wound area was viewed and photographed at 0 and 24 h after scratching. Cell migration rate was calculated as follows: (original gap distance -current gap distance)/original gap distance x100%. Transwell migration and invasion assays were examined using 24-well chambers (8 $\mu$m Transwell filters per chamber) (Corning Inc., Corning, MA, USA). Then, $3x10^4$ cells in 200 $\mu$l serum-free medium were added to the upper chamber containing an uncoated or Matrigel-coated (BD Biosciences, San Jose, CA, USA) membrane. The lower chamber contained 600 $\mu$l culture medium supplemented with 20% FBS. After being cultured for 24 h in an incubator, cells on the upper surface of the microporous membrane were wiped off with a cotton swab, fixed with 4% paraformaldehyde for 20 min, and stained with 0.1% crystal violet for 30 min. Migrated or invaded cells were counted in five randomly chosen fields in each chamber. Imaging and counting were performed at x200 magnification under a light microscope. The experiments were executed in triplicate.

*Subcutaneous and peritoneal xenograft tumor models*. BALB/c-nu mice, 4-6 weeks old, were purchased from Hunan SJA Laboratory Animal Company (Changsha, China). All animal protocols were approved by the Ethics Committee of Jiangxi Province People's Hospital. Five mice were divided randomly into each group. To explore the effects of *CHD1L* on tumor growth and metastasis *in vivo*, $1x10^7$ cells were injected into the left axilla and enterocoelia of the mice (17,18) (5 mice/group). Tumor growth was observed every week and measured in two dimensions. The tumor volume (V) was calculated using the following formula: $V=4\pi/3 \times (width/2)^2 \times (length/2)$. After 4 weeks, the mice were sacrificed under cervical dislocation and the tumors were dissected out and weighed. Then, metastatic tumors were fixed with formalin and embedded in paraffin. Finally, the expression levels of *CHD1L*, E-cadherin and N-cadherin were evaluated by IHC.

*Statistical analysis*. GraphPad Prism 6.0 software (GraphPad Software, Inc., Chicago, IL. USA) was used to process data and images. Each experimental value was expressed as the mean ± standard deviation (SD). The paired Student's t-test mainly applies to *CHD1L* protein levels in tumor and

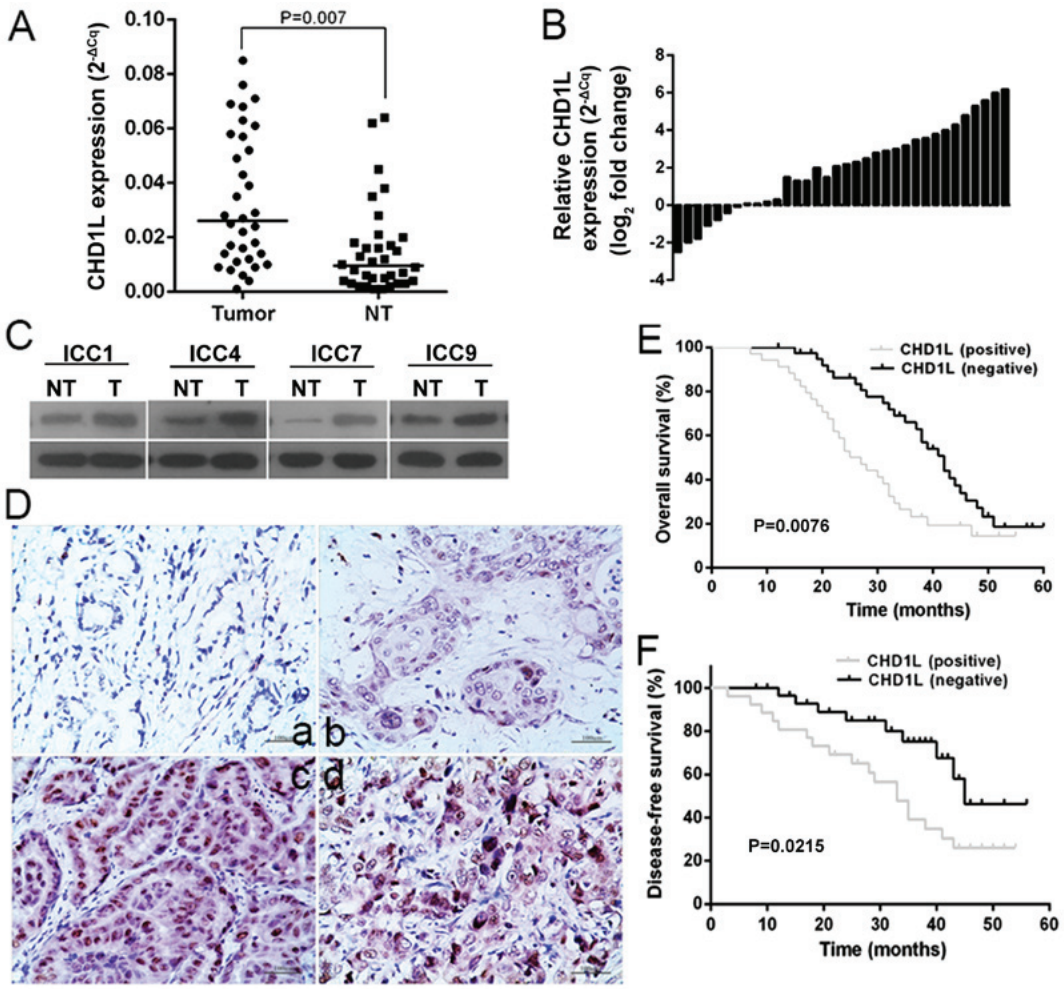


Figure 1. Expression of *CHD1L* is upregulated and correlated with poor prognosis in ICC. (A) The mRNA expression of *CHD1L* in 34 ICC tissues (T) compared to the corresponding adjacent non-tumor tissues (NT) determined by RT-qPCR (P=0.007). *GADPH* was used as the internal control. (B) Comparison of the *CHD1L* expression level between ICC tissues and their paired non-tumor tissues. The relative *CHD1L* expression was calculated as the Tumor/NT expression ratio ($2^{-\Delta\Delta Cq}$). (C) The protein expression of *CHD1L* in ICC tissues (T) and their paired non-tumor tissues (NT) was detected by western blotting. (D) IHC analysis of *CHD1L* protein expression in the specimens. Nuclear staining of *CHD1L* (brown) was detected in tumor tissue. (a) Hepatolithiasis tissues, *CHD1L*(-); (b) well-differentiated ICC specimen, *CHD1L*(+); (c) moderately differentiated ICC specimen, *CHD1L* (++); and (d) poorly differentiated ICC specimen, *CHD1L*(+++). Scale bar, 100 $\mu$m. (E and F) Kaplan-Meier survival analysis of the correlation between *CHD1L* expression and ICC patient overall and disease-free survival (log-rank, 7.117; P=0.0076) (log-rank, 5.285; P=0.0215). *CHD1L*, chromodomain helicase/ATPase DNA-binding protein 1-like gene; ICC, intrahepatic cholangiocarcinoma.

adjacent non-tumor tissues. The Chi-square ($\chi^2$) test was used to analyze the association of *CHD1L* expression with the clinicopathological characteristics of ICC. Kaplan-Meier plots and log-rank tests were used for survival analysis. Univariate and multivariate Cox proportional hazard regression models were used to analyze independent prognostic factors. P<0.05 was considered statistically significant, and all assays were performed in triplicate independent experiments.

## Results

*Expression of CHD1L is upregulated and is correlated with a poor prognosis in ICC*. To assess the potential role of *CHD1L* in ICC, we used RT-qPCR and western blotting to measure the expression of *CHD1L* in 34 fresh clinical ICC tissues and their paired adjacent non-tumor tissues. The relative expression level of *CHD1L* in ICC tissues was significantly higher than that noted in the paired adjacent non-tumor tissues (P=0.007; Fig. 1A and B). Consistent with the RT-qPCR results, significantly increased *CHD1L* protein levels were observed in the ICC tissues, when compared with the matched adjacent non-cancerous tissues (P<0.01; Fig. 1C). Furthermore, protein expression levels of *CHD1L* were measured in 80 samples of stored paraffin-embedded ICC tissues and 30 hepatolithiasis tissues by immunohistochemistry (Fig. 1D). *CHD1L* was overexpressed in tumor tissues compared with that noted in hepatolithiasis tissues (P=0.03, Table III). Then, the clinical significance of *CHD1L* overexpression in the ICC cohort was investigated by statistical analysis. We found that *CHD1L* overexpression was closely related to histological differentiation (P=0.011), vascular invasion (P=0.002), lymph node metastasis (P=0.008) and TNM stage (P=0.001), suggesting that *CHD1L* may play roles in ICC metastasis (Table IV). Kaplan-Meier analysis showed that ICC patients with positive *CHD1L* expression had reduced overall and disease-free survival than those with negative *CHD1L* expression (log rank, 7.117; P=0.0076; Fig. 1E) (log rank, 5.285; P=0.0215; Fig. 1F). Cox regression statistical analysis was used to test the effects of

Table III. Immunohistochemical analysis of CHD1L protein expression in the specimens.

| Groups | N | CHD1L expression | | | | P-value |
|---|---|---|---|---|---|---|
| | | Negative (0-1) | Weak (2-3) | Moderate (4-6) | Strong (6-9) | |
| Intrahepatic cholangiocarcinoma | 80 | 16 | 28 | 15 | 21 | 0.03 |
| Hepatolithiasis | 30 | 15 | 8 | 5 | 2 | |

CHD1L, chromodomain helicase/ATPase DNA-binding protein 1-like gene.

Table IV. Correlation between CHD1L expression and the clinicopathological features of 80 patients with ICC.

| Clinicopathological features | No. | CHD1L | | $\chi^2$ value | P-value |
|---|---|---|---|---|---|
| | | High n (%) | Low n (%) | | |
| Total cases | 80 | 36 (45.0) | 44 (55.0) | | |
| Sex | | | | 0.522 | 0.47 |
| Male | 49 | 23 (46.9) | 26 (53.1) | | |
| Female | 31 | 12 (38.7) | 19 (61.3) | | |
| Age (years) | | | | 1.204 | 0.273 |
| ≥55 | 46 | 20 (43.5) | 26 (56.5) | | |
| <55 | 34 | 19 (55.9) | 15 (44.1) | | |
| Histological differentiation | | | | 8.973 | 0.011[a] |
| Well | 23 | 7 (30.4) | 16 (69.6) | | |
| Moderate | 42 | 20 (47.6) | 22 (52.4) | | |
| Poor | 15 | 12 (80.0) | 3 (20) | | |
| Tumor size (cm) | | | | 2.161 | 0.142 |
| ≥4.0 | 52 | 33 (63.5) | 19 (36.5) | | |
| <4.0 | 28 | 13 (46.4) | 15 (53.6) | | |
| Vascular invasion | | | | | |
| Present | 36 | 23 (63.9) | 13 (36.1) | 9.436 | 0.002[a] |
| Absent | 44 | 13 (29.5) | 31 (70.5) | | |
| CA19-9 (U/ml) | | | | 0.671 | 0.413 |
| ≥35 | 45 | 26 (57.8) | 19 (42.2) | | |
| <35 | 35 | 17 (48.6) | 18 (51.4) | | |
| Lymphatic node metastasis | | | | 7.026 | 0.008[a] |
| Present | 48 | 31 (64.6) | 17 (35.4) | | |
| Absent | 32 | 11 (34.4) | 21 (35.6) | | |
| TNM stage (AJCC) | | | | 14.831 | 0.001[a] |
| I-II | 30 | 6 (20.0) | 24 (80.0) | | |
| III | 36 | 19 (52.8) | 17 (47.2) | | |
| IV | 14 | 11 (78.6) | 3 (21.4) | | |

CHD1L, chromodomain helicase/ATPase DNA-binding protein 1-like gene; ICC, intrahepatic cholangiocarcinoma. [a]P<0.05 is significant.

*CHD1L* on the independent prognostic value of ICC patients. Overexpression of the *CHD1L* protein, as well as other clinicopathological variables (histological differentiation, vascular invasion, lymph node metastasis and TNM stage) that showed significance by univariate analysis (all P<0.05; Table V), were included in the multivariate analysis (hazard ratio, 5.875; 95% confident interval: 3.243-8.023, P<0.001; Table V). The *CHD1L* protein was identified as an independent prognostic factor for poor overall and disease-free survival in ICC patients. Taken together, these results revealed that *CHD1L* was aberrantly

Table V. Univariate and multivariate analyses of the different prognostic variables in the ICC patients.

| | Univariate analysis | | | Multivariate analysis | | |
|---|---|---|---|---|---|---|
| Variable | HR | 95% CI | P-value | HR | 95% CI | P-value |
| CHD1L | 4.852 | 1.758-8.758 | <0.001[a] | 5.875 | 3.243-8.023 | <0.001[a] |
| Sex | 1.356 | 0.475-2.354 | 0.123 | | | |
| Age | 0.875 | 0.652-1.102 | 0.763 | | | |
| Histologic differentiation | 3.142 | 1.246-5.863 | <0.001[a] | | | |
| Tumor size | 0.968 | 0.389-1.821 | 0.369 | | | |
| Vascular invasion | 8.257 | 3.012-13.562 | <0.001[a] | | | |
| CA-199 | 1.102 | 0.526-1.956 | 0.425 | | | |
| Lymphatic node metastasis | 4.232 | 1.897-8.014 | 0.0035[a] | 3.653 | 1.536-8.524 | 0.016[a] |
| TNM stage (AJCC) | 4.452 | 1.356-7.485 | <0.001[a] | 4.265 | 1.875-9.231 | 0.002[a] |

CHD1L, chromodomain helicase/ATPase DNA-binding protein 1-like gene; ICC, intrahepatic cholangiocarcinoma; CI, confidence interval; HR, hazard ratio. [a]P<0.05 is significant.

overexpressed in ICC tissues, and this overexpression was associated with ICC progression.

*CHD1L is overexpressed in ICC cell lines*. To further explore the role of *CHD1L* in the progression of ICC, we examined the expression of *CHD1L* in one normal bile duct epithelial cell line (HiBECs) and four ICC cell lines (HCCC9810, RBE, QBC939 and HuCCT1) by western blotting and RT-qPCR. The results showed that the protein levels of *CHD1L* were relatively higher in ICC cell lines when compared to HiBECs, especially in RBE and HuCCT1 (Fig. 2A). Consistent mRNA levels were observed in RT-qPCR (Fig. 2B). We chose RBE and HUCCT1 cell lines for stable transfection with *CHD1L*-shRNA lentivirus vectors, and we chose HCCC9810 cell lines for stable transfection with *CHD1L*-overexpression plasmid vector. We detected the transduction efficiency by EGFP expression under a fluorescence microscope at 36-48 h after transduction. The efficiency of lentiviral transduction in both RBE and HUCCT1 cell lines was higher than 85%. The transfection efficiency was further confirmed by western blotting (Fig. 2C) and RT-qPCR (Fig. 2D). Our results showed that the effect of shRNA transduction on the expression of *CHD1L* was examined using western blotting and RT-qPCR analysis with the most efficient knockdowns by *shCHD1L-1* in RBE and HUCCT1 cell lines compared with those of the other two vectors (*shCHD1L-2* and *shCHD1L-3*), and the expression of *CHD1L* in the control group (CTRL) and the shNC groups were significantly higher than in the *CHD1L*-silenced group. In addition, the expression of *CHD1L* with *CHD1L*-expression plasmid vector in HCCC9810 cell lines was significantly higher than that in the empty vector-transfected cell (MOCK) group and the control (CRTL).

*CHD1L has strong tumorigenic function*. As previously reported, *CHD1L* may show pro-cancer effects. Therefore, the tumorigenic ability of *CHD1L* was evaluated by CCK-8 and plate colony formation assays *in vitro*. A CCK-8 assay showed that the proliferative capacity of the *shCHD1L-1* transfected group was clearly gradually inhibited compared with the control group at 48, 72 and 96 h in the RBE and HUCCT1 ICC cell lines (Fig. 3A). Additionally, as compared with the shNC and CTRL groups, plate colony formation assays demonstrated that the number of colonies formed by RBE and HUCCT1 ICC cell lines was significantly reduced by *CHD1L* depletion (Fig. 3B). Moreover, to assess the tumorigenicity of *CHD1L in vivo*, tumor formation in nude mice was performed by injecting *CHD1L*-knockdown or control RBE cells into the right back of 5 nude mice, respectively. Then, the tumor volume was calculated. The results showed that the tumors formed in the *CHD1L*-silencing xenografts were significantly smaller than that noted in the control (CTRL) cells (Fig. 3C). In contrast, compared with the MOCK and CRTL, *CHD1L*-transfected HCCC9810 cells showed a stronger proliferation rate (Fig. 3A) and increased numbers of colony forming units (Fig. 3B). In total, these results indicated that overexpression of *CHD1L* had strong tumorigenic ability.

*Overexpression of CHD1L promotes G1/S phase transition*. To investigate the effect of *CHD1L* on cell cycle distribution, we evaluated alterations in the cell cycle phase after treatment with the *CHD1L*-knockdown lentivirus by flow cytometry. As shown in the results, cells in the G1 phase increased, while cells in the S phase decreased in the *shCHD1L-1* cells, compared with control cells and shNC (P<0.05; Fig. 4A and B). This finding indicated that inhibition of *CHD1L* could obstruct G1/S cell cycle transition. To further confirm the results, *CHD1L*-overexpression vector was transfected into HCCC9810 cells. The MOCK and CRTL groups were used as control. The results showed that the percentages of cells in the G1 and S phases were significantly decreased and increased, respectively, in the *CHD1L*-overexpression cells, compared with cells in the MOCK and CRTL groups (P<0.05; Fig. 4C). To further explore the mechanisms of *CHD1L* in promoting G1/S phase transition, the effects of *CHD1L* on cell cycle regulators, namely, *P53*, *cyclin D1* and *CDK2*, were examined by western blotting. As shown in the results, *P53* expression was upregulated while *CDK2* and *cyclin D1* were downregulated in the

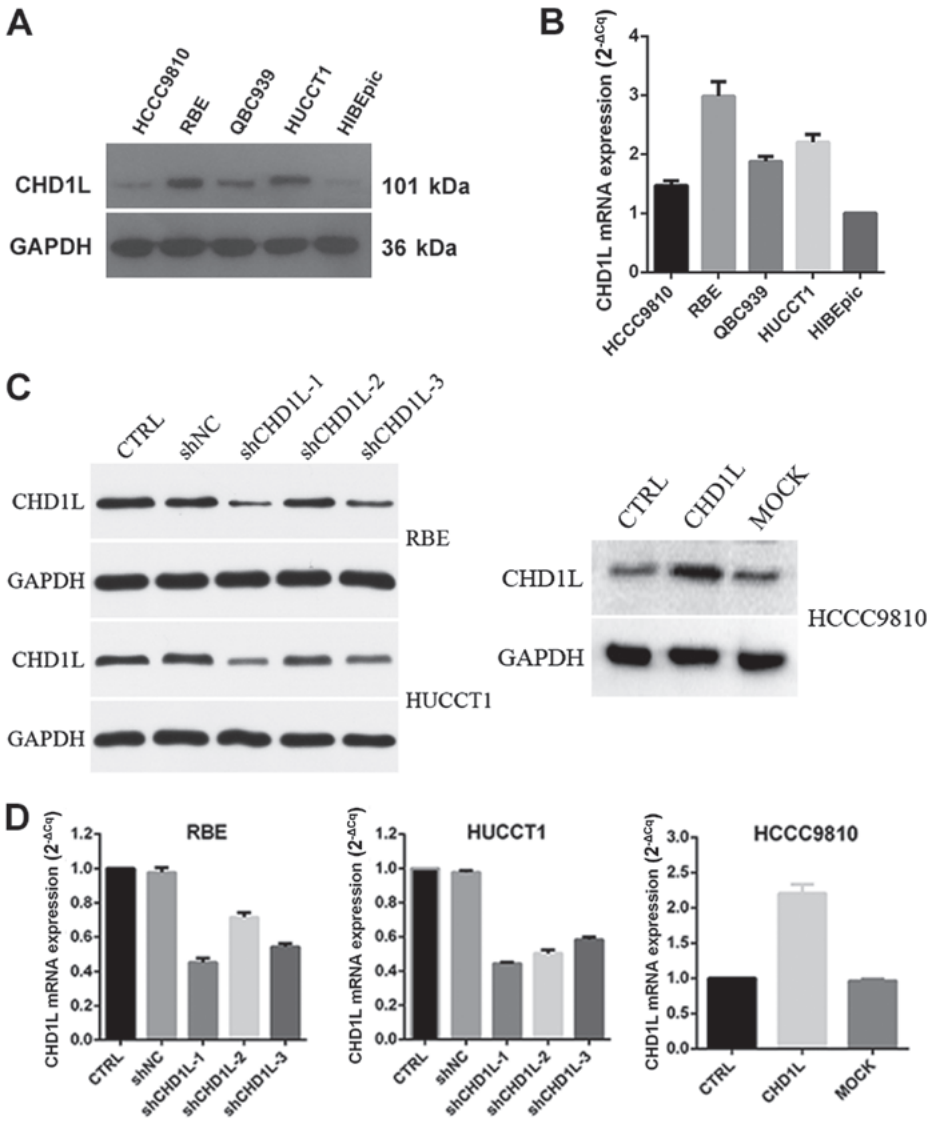


Figure 2. *CHD1L* expression in ICC cell lines. (A and B) Protein and mRNA expression of *CHD1L* in normal epithelial cells, HiBECs, and ICC cell lines HCCC9810, RBE, QBC939 and HuCCT1. (C and D) Transduction efficiency of *CHD1L* expression in *CHD1L*-silenced RBE and HUCCT1 cells (sh*CHD1L*-1, -2 and -3) and *CHD1L*-overexpressing HCCC9810 cells (*CHD1L*) was examined by western blotting and RT-qPCR. *GAPDH* was used as the loading control. *CHD1L*, chromodomain helicase/ATPase DNA-binding protein 1-like gene; ICC, intrahepatic cholangiocarcinoma; CTRL, control; MOCK, empty vector-transfected cells; shNC, negative control.

*shCHD1L-1* group in RBE cells whereas *P53* expression was downregulated and *CDK2* and *cyclin D1* were upregulated in the *CHD1L*-overexpressing HCCC9810 cells (Fig. 4D). This finding indicated that *CHD1L* may promote G1/S transition by affecting critical cell cycle proteins.

*CHD1L increases ICC cell migration and invasion by inducing EMT.* To study the role of *CHD1L* in ICC cell migration and invasion, we applied wound healing, Transwell migration and Matrigel invasion assays *in vitro*. The wound healing assay showed that the rate of motility was significantly decreased in RBE and HUCCT1 cells by *CHD1L*-depletion compared to the CTRL and shNC groups, while overexpression of *CHD1L* in HCCC9810 cells showed the opposite effect (P<0.001; Fig. 5A). Similarly, Transwell migration and Matrigel invasion assays demonstrated that the cells number of migration and invasion of the CTRL and shNC groups were significantly more than the treated group. Conversely, the invasiveness of the *CHD1L*-expressing cells was significantly higher than CTRL and MOCK cells (P<0.0001; Fig. 5B). Therefore, these results suggest that *CHD1L* increases ICC cell migration and invasion. To explore whether *CHD1L* promotes the invasiveness of ICC through EMT, we examined EMT-related biomarkers by western blotting (Fig. 5C). The result showed that RBE and HUCCT1 cells transfected with *shCHD1L* expressed high levels of E-cadherin, which is characteristic of epithelial cells. However, in ICC cell lines transfected with *shCHD1L*, expression levels of proteins related to the mesenchymal phenotype (N-cadherin and vimentin) were downregulated. Overexpression of *CHD1L* could reverse this phenotype in HCCC9810 cells. These results indicated that *CHD1L* increased ICC cell migration and invasion by inducing EMT.

*CHD1L promotes tumor metastasis in BALB/c-nu mice via mesenchymal-epithelial transition (MET).* To confirm the *in vivo* effects of *CHD1L* on metastasis, we performed a liver metastasis

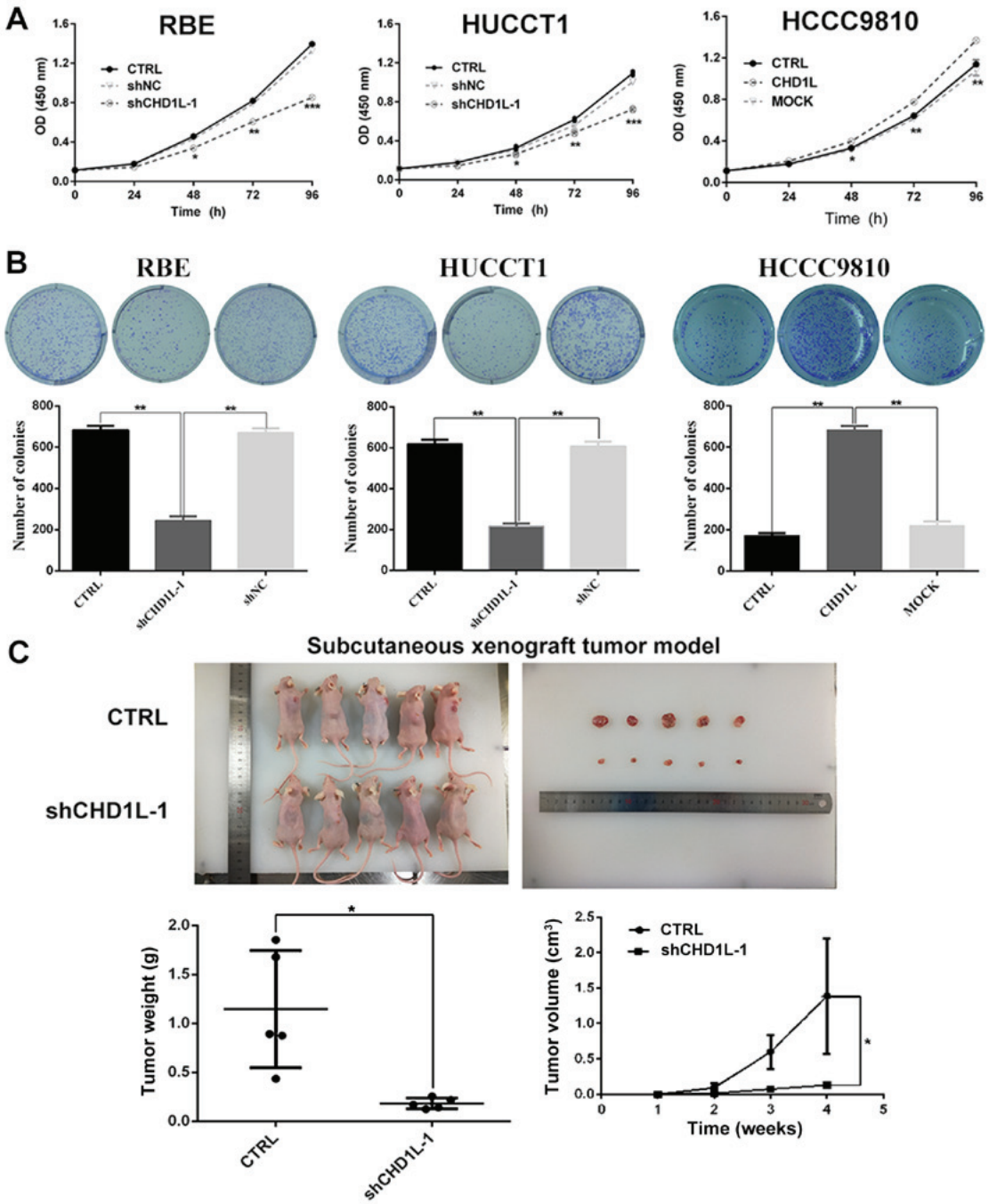


Figure 3. *CHD1L* exhibits strong tumorigenic function. (A) Cell growth rates were calculated by CCK-8 proliferation assays at various time-points ($^{*}$P<0.05, $^{**}$P<0.01 and $^{***}$P<0.001). (B) Representative images of colony formation in the CTRL, *CHD1L* knockdown (sh*CHD1L*-1) and shNC groups in RBE and HUCCT1 cells and in the CTRL, *CHD1L*-overexpressing (*CHD1L*) and MOCK groups in HCCC9810 cells. The numbers of colonies were calculated and are documented in the bar chart ($^{**}$P<0.01). (C) Representative images of tumors formed in nude mice injected with the indicated RBE cells. A statistical plot of average tumor weights in the subcutaneous xenograft tumor model. Tumor growth curves are shown in the line chart ($^{*}$P<0.05). *CHD1L*, chromodomain helicase/ATPase DNA-binding protein 1-like gene; CCK-8, Cell Counting Kit-8; CTRL, control; MOCK, empty vector-transfected cells; shNC, negative control.

model with BALB/c-nu mice *in vivo* after inoculation with *shCHD1L-1* or CTRL-transfected cells. The RBE cell suspension was injected into the abdominal cavity of nude mice. After the peritoneal metastatic tumors grew, the mice were euthanized and the livers were harvested (Fig. 6A). Metastatic liver tumors were observed in 2 of 5 and 4 of 5 *shCHD1L-1*- and CTRL-injected nude mice, respectively (Table VI). To determine whether MET plays a role in tumor metastasis induced by CHD1L in the nude mouse, IHC with antibodies against E-cadherin and N-cadherin was performed on serial sections of each tumor (Fig. 6B). The IHC results showed that decreased expression of E-cadherin and increased expression of N-cadherin were observed in tumors induced by *shCHD1L-1* cells compared with tumors induced by CTRL cells. This suggests that the *CHD1L* promotes ICC metastasis *in vivo* by MET.

## Discussion

In a previous study, a candidate oncogene chromodomain helicase/ATPase DNA-binding protein 1-like gene (*CHD1L*)

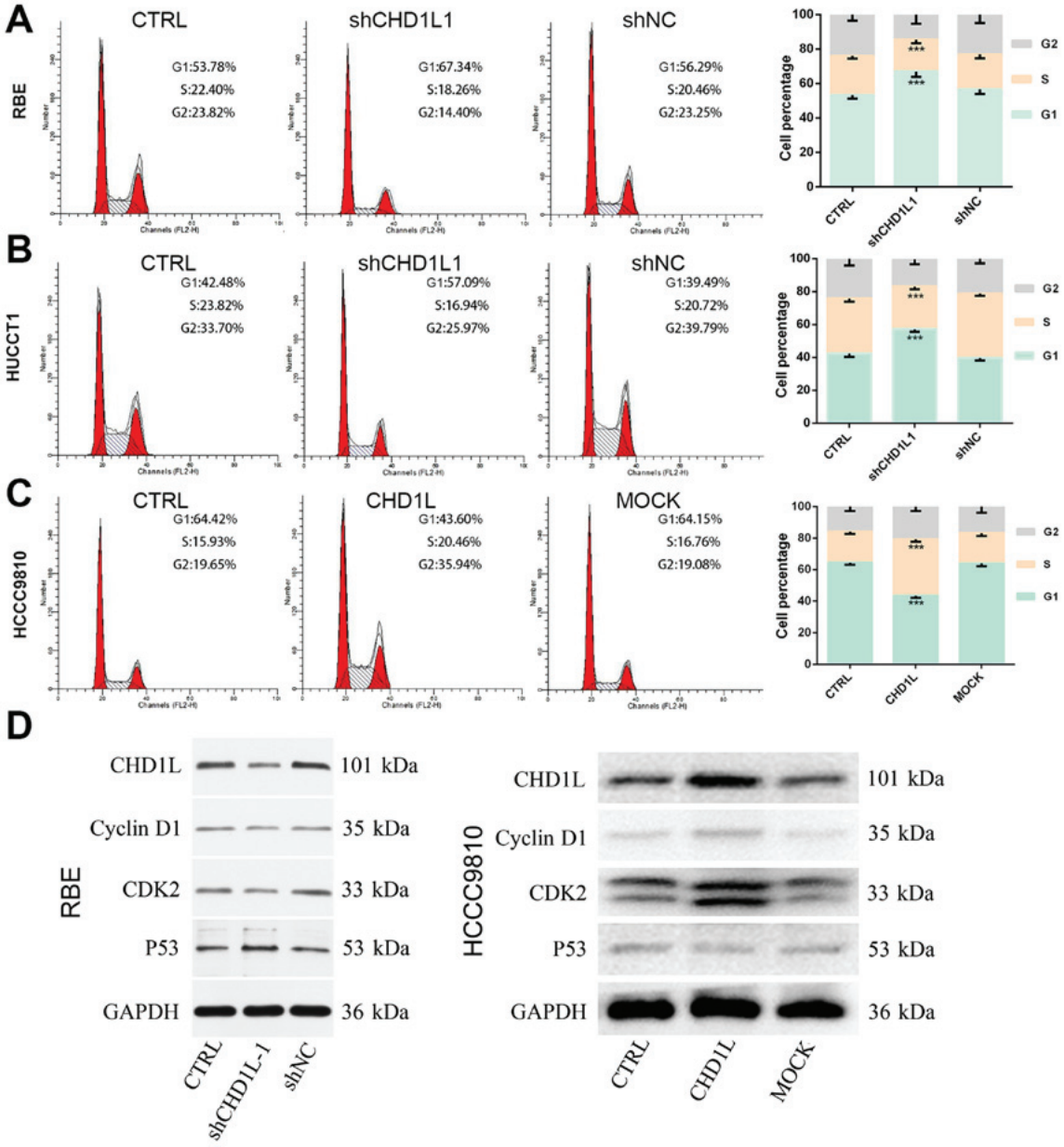


Figure 4. Overexpression of *CHD1L* promotes G1/S phase transition. (A and B) Flow cytometry was used to compare cell cycle distribution in the CTRL, *CHD1L* knockdown (*shCHD1L-1*) and shNC groups. The percentages of cells at G1, S and G2 phase are summarized in the bar charts. Data are shown as the mean ± SD of three independent experiments (***P<0.001; independent Student's t-test). (C) Overexpression promoted a smaller proportion of cells in the G1 stage and a higher proportion of cells in the S phase of the cell cycle. Data are shown as the mean ± SD of three independent experiments (***P<0.001; independent Student's t-test). (D) The protein expression of P53, cyclin D1 and CDK2 was observed by western blotting in *CHD1L*-silenced RBE (left panel) and *CHD1L*-overexpressing HCCC9810 (right panel) cell lines. *CHD1L*, chromodomain helicase/ATPase DNA-binding protein 1-like gene; CTRL, control; MOCK, empty vector-transfected cells; shNC, negative control.

was identified in hepatocellular carcinoma (HCC) (6). It is overexpressed in many tissues, including the bladder (19) and colorectal cancer (20), glioma (21), myeloma (22) and lung adenocarcinoma (23). Recently, *CHD1L* expression was found to increase tumor progression in pancreatic cancer (24). Although *CHD1L* is reported to be overexpressed in several other types of carcinoma, it has not been linked to intrahepatic cholangiocarcinoma (ICC). In the present study, we aimed to detect *CHD1L* expression in tumor tissues and evaluate its prognostic significance in ICC. Our results showed that *CHD1L* was overexpressed in ICC tissues compared with the adjacent non-tumor tissues, indicating that *CHD1L* may have an effect on ICC development. Moreover, IHC results demonstrated that overexpression of *CHD1L* was significantly related to histological differentiation, vascular invasion, lymph node metastasis, TNM stage and a shorter overall and disease-free survival time of ICC patients. In addition, Cox regression statistical analysis further indicated that high *CHD1L* expression was an independent predictor for poor prognosis in ICC patients. Therefore, *CHD1L* overexpression in ICC may serve as a biomarker for early diagnosis and precise prognoses.

Additionally, we evaluated the expression of *CHD1L* in ICC cell lines by western blotting and RT-qPCR. The expression level of *CHD1L* was relatively higher in ICC cell lines than that in HiBECs and the normal bile duct epithelial cell line, which suggested that *CHD1L* may have oncogenic ability. Meanwhile,

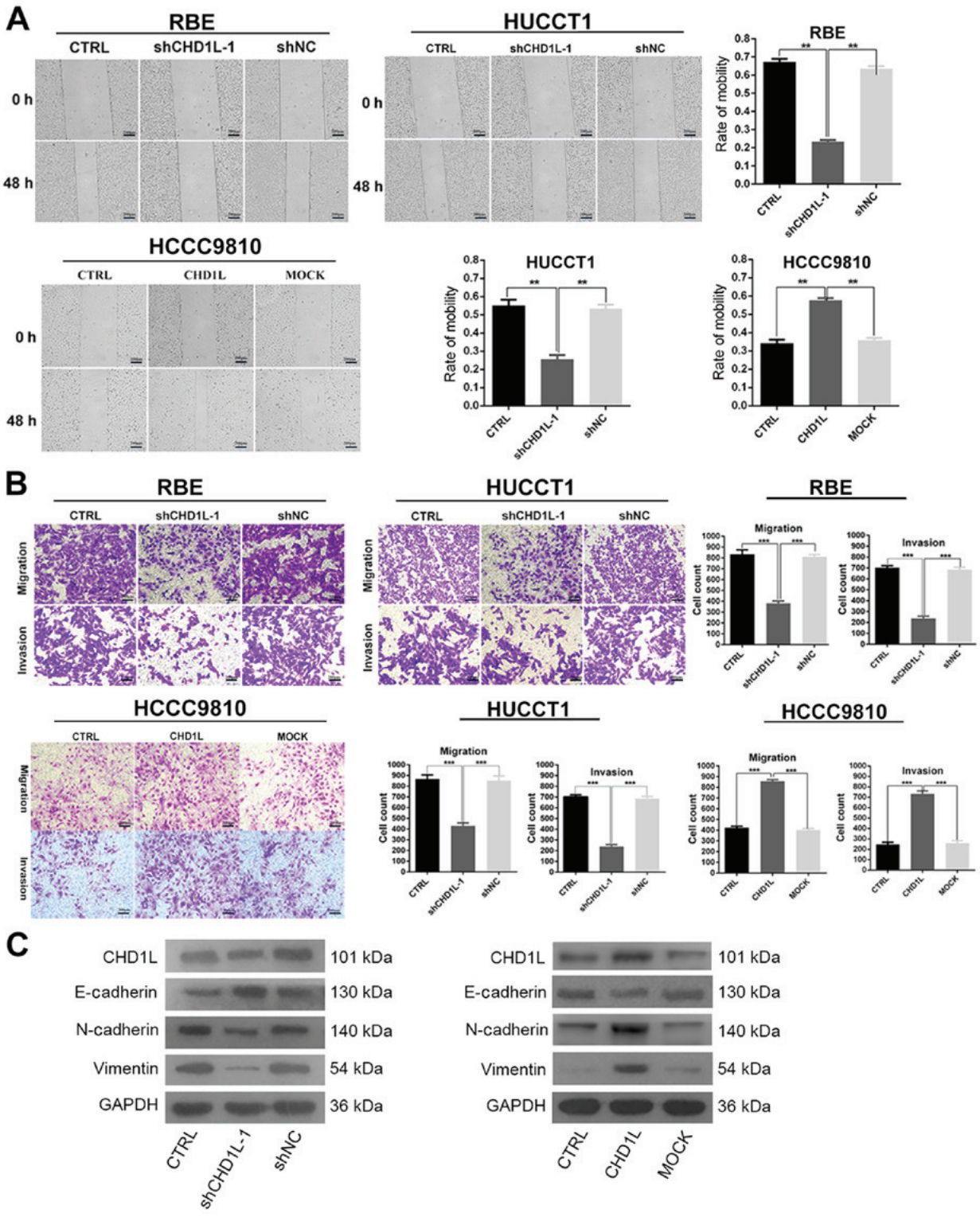


Figure 5. *CHD1L* increases ICC cell migration and invasion by inducing EMT. (A) Cell migration ability in RBE, HUCCT1 and HCCC9810 cells in the various groups was detected at 48 h by wound healing assay. The rate of mobility was calculated and is depicted in the bar chart ($^{**}$P<0.01). Scale bar, 200 $\mu$m. (B) Transwell migration and invasion assays demonstrated that the number of migrated and invasive cells in the *CHD1L*-knockdown (*shCHD1L-1*) groups were significantly reduced compared with the other two groups in RBE and HUCCT1 cells. Overexpression of *CHD1L* in the HCCC9810 cells had the opposite effects ($^{***}$P<0.001). Scale bar, 200 $\mu$m. (C) The protein expression of EMT-related biomarkers (vimentin, N-cadherin and E-cadherin) in the indicated cells was examined by western blotting. *CHD1L*, chromodomain helicase/ATPase DNA-binding protein 1-like gene; ICC, intrahepatic cholangiocarcinoma; EMT, epithelial-mesenchymal transition; CTRL, control; MOCK, empty vector-transfected cells; shNC, negative control.

the highest *CHD1L* levels were found in highly aggressive cell lines RBE (25) and HUCCT1 (26) and the lowest *CHD1L* levels were found in ICC cell line HCCC9810 (27). Hence, we chose RBE and HUCCT1 cell lines for stable transfection with *CHD1L*-shRNA lentivirus vectors, and HCCC9810 cell lines for stable transfection with the *CHD1L*-overexpression plasmid vector. Our results demonstrated the effect of shRNA transduction on the expression of *CHD1L* and the most efficient

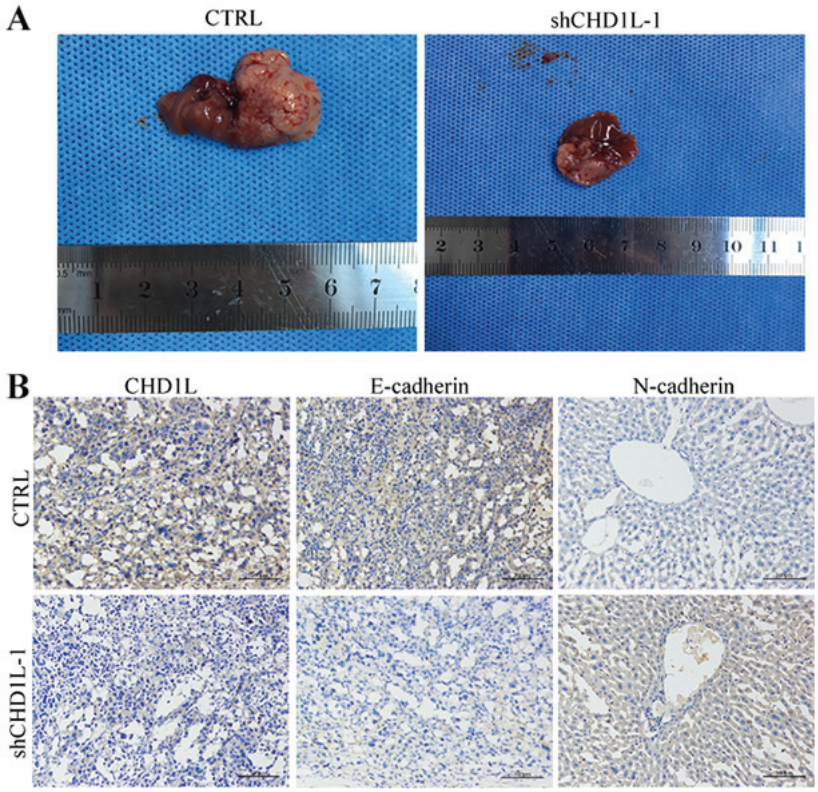


Figure 6. *CHD1L* promotes tumor metastasis in BALB/c-nu mice via mesenchymal-epithelial transition (MET). (A) A metastasis assay *in vivo* was performed to evaluate the effect of *CHD1L*-silenced (*shCHD1L-1*) cells on tumor metastasis. (B) Immunohistochemical staining of *CHD1L*, E-cadherin and N-cadherin in tumor tissues of the metastasis model. Scale bar, 100 $\mu$m. *CHD1L*, chromodomain helicase/ATPase DNA-binding protein 1-like gene; CTRL, control.

Table VI. Tumor incidence rate during the 4-week observation period between CTRL and shCHD1L-1.

| | Tumor incidence rate (n/total) for week | | | |
|---|---|---|---|---|
| Groups | 1 | 2 | 3 | 4 |
| CTRL | 0/5 | 1/5 | 3/5 | 4/5 |
| shCHD1L-1 | 0/5 | 0/5 | 1/5 | 2/5 |

CHD1L, chromodomain helicase/ATPase DNA-binding protein 1-like gene; CTRL, control.

knockdown by *shCHD1L-1* was noted when compared with those of the other two vectors *(shCHD1L-2* and *shCHD1L-3*).

In addition, promotion of cell proliferation is a major molecular mechanism of an oncogene in cancer development. In the present study, we demonstrated that *CHD1L* had strong tumorigenic ability *in vitro* and *in vivo* functional studies. Inhibition of *CHD1L* obstructed G1/S cell cycle transition and the effect was reversed by *CHD1L* overexpression. *P53* is crucial for effective tumor suppression in humans (28) and can upregulate the expression of *P21*, which in turn functions as a *CDK2* inhibitor to control S phase entry via the inactivation of the *cyclin D1-CDK2* complex (29,30). Consistent with this theory, we found that *CHD1L* reduced *P53* expression and increased S-phase-specific protein expression, including *CDK2* and *cyclin D1,* after *CHD1L*-overexpression transfection. This evidence suggested that the dysregulation of the *P53/cyclin D1/CDK2* pathway maybe involved in *CHD1L*-induced G1/S transition in ICC.

Finally, we found that *CHD1L* promoted ICC cell migration and invasion, suggesting that *CHD1L* may promote metastasis-related genetic alterations in ICC cells. It has been reported that metastasis is the most common cause of death from malignant neoplasms (31). Metastasis is a multistep cellular process by which tumor cells disseminate from their primary site and form secondary tumors at a distant site. The pathophysiological course of metastasis is mediated by the dynamic plasticity of cancer cells, which enables them to shift between epithelial and mesenchymal phenotypes through a transcriptionally regulated program termed EMT and its reverse process MET (32). EMT includes loss of cell-cell adhesion and activation of mesenchymal markers, as well as increased motility of tumor cells (33). It has been reported that *CHD1L* promotes HCC progression and metastasis by induction of EMT (34). In the present study, we found that inhibition of the expression of *CHD1L* induced EMT by upregulation of expression of the epithelial marker, E-cadherin, and downregulation of expression of the mesenchymal markers, N-cadherin and vimentin. Furthermore, silencing of *CHD1L* expression inhibited MET phenotype, which involved decreased expression of E-cadherin and increased expression of N-cadherin in nude mice by IHC. Our findings indicate that *CHD1L* may drive EMT and MET in cancer cells, resulting in metastasis.

In summary, we confirmed that the overexpression of *CHD1L* was associated significantly with histological differentiation, vascular invasion, lymph node metastasis, TNM

stage, and the shorter overall and disease-free survival time of ICC patients. *CHD1L* promotes ICC cell proliferation and metastasis both *in vitro* and *in vivo*. We hypothesize that the dysregulation of the *P53/cyclin D1/CDK2* pathway maybe involved in *CHD1L*-induced G1/S transition and that *CHD1L* may drive EMT and MET in ICC cells, resulting in metastasis. Taken together, this study offers new insights that *CHD1L* may serve as an oncogene in ICC pathogenesis. However, our research has some shortcomings. First, further research is still needed to validate the more reasonable approach to silence or overexpress *CHD1L*. Second, a better understanding of the oncogenic mechanisms of *CHD1L* during ICC initiation and progression may have implications for future patient treatment.

**Acknowledgements**

The authors thank the Key Molecular Medical Laboratory of Jiangxi Province (Nanchang, China) for providing the technical assistance, and offering human intrahepatic biliary epithelial cells (HiBECs).

**Funding**

The present study was supported by the Natural Science Foundation of Jiangxi Province, China (grant no. 20151512070090), the Science and Technology Program of Health and Planning Commission in Jiangxi Province (grant no. 20161048) and the Science and Technology Research of Education Department in Jiangxi Province (grant no. GJJ150049).

**Availability of data and materials**

The datasets used during the present study are available from the corresponding author upon reasonable request.

**Authors' contributions**

SL and YC were responsible for the experimental design. SL contributed to the execution of the experiments, data statistical analysis and the manuscript content. YC and YD participated in performing the experiments and in the manuscript mapping and submission. TY participated in the writing of the Discussion and data interpretation. CW conceived the study and revised the manuscript. CH was responsible for the funding application, the supervision and management of the project and offered technical instruction and assistance. All authors read and approved the manuscript and agree to be accountable for all aspects of the research in ensuring that the accuracy or integrity of any part of the work are appropriately investigated and resolved.

**Ethics approval and consent to participate**

All procedures in studies were in accordance with the ethical standards of the Human Biomedical Research and Animal Research Ethics Review Board of the People's Hospital of Jiangxi Provincial (Nanchang, China). Informed consent was obtained from all individual participants included in this study.

**Patient consent for publication**

Not applicable.

**Competing interests**

The authors state that they have no competing interests.

**References**

1. Siegel RL, Miller KD and Jemal A: Cancer statistics, 2016. CA Cancer J Clin 66: 7-30, 2016.
2. Wang Y, Li J, Xia Y, Gong R, Wang K, Yan Z, Wan X, Liu G, Wu D, Shi L, *et al*: Prognostic nomogram for intrahepatic cholangiocarcinoma after partial hepatectomy. J Clin Oncol 31: 1188-1195, 2013.
3. Haga H and Patel T: Molecular diagnosis of intrahepatic cholangiocarcinoma. J Hepatobiliary Pancreat Sci 22: 114-123, 2015.
4. Bridgewater J, Galle PR, Khan SA, Llovet JM, Park JW, Patel T, Pawlik TM and Gores GJ: Guidelines for the diagnosis and management of intrahepatic cholangiocarcinoma. J Hepatol 60: 1268-1289, 2014.
5. Okumura S, Kaido T, Hamaguchi Y, Kobayashi A, Shirai H, Fujimoto Y, Iida T, Yagi S, Taura K, Hatano E, *et al*: Impact of skeletal muscle mass, muscle quality, and visceral adiposity on outcomes following resection of intrahepatic cholangiocarcinoma. Ann Surg Oncol 24: 1037-1045, 2017.
6. Ma NF, Hu L, Fung JM, Xie D, Zheng BJ, Chen L, Tang DJ, Fu L, Wu Z, Chen M, *et al*: Isolation and characterization of a novel oncogene, amplified in liver cancer 1, within a commonly amplified region at 1q21 in hepatocellular carcinoma. Hepatology 47: 503-510, 2008.
7. Cheng W, Su Y and Xu F: CHD1L: A novel oncogene. Mol Cancer 12: 170, 2013.
8. Chen L, Yuan YF, Li Y, Chan TH, Zheng BJ, Huang J and Guan XY: Clinical significance of CHD1L in hepatocellular carcinoma and therapeutic potentials of virus-mediated CHD1L depletion. Gut 60: 534-543, 2011.
9. Wu J, Zong Y, Fei X, Chen X, Huang O, He J, Chen W, Li Y, Shen K and Zhu L: Presence of CHD1L over-expression is associated with aggressive tumor biology and is a novel prognostic biomarker for patient survival in human breast cancer. PLoS One 9: e98673, 2014.
10. Su Z, Zhao J, Xian G, Geng W, Rong Z, Wu Y and Qin C: CHD1L is a novel independent prognostic factor for gastric cancer. Clin Transl Oncol 16: 702-707, 2014.
11. Su FR, Ding JH, Bo L and Liu XG: Chromodomain helicase/ATPase DNA binding protein 1-like protein expression predicts poor prognosis in nasopharyngeal carcinoma. Exp Ther Med 8: 1745-1750, 2014.
12. He WP, Zhou J, Cai MY, Xiao XS, Liao YJ, Kung HF, Guan XY, Xie D and Yang GF: CHD1L protein is overexpressed in human ovarian carcinomas and is a novel predictive biomarker for patients survival. BMC Cancer 12: 437, 2012.
13. Farges O, Fuks D, Le Treut YP, Azoulay D, Laurent A, Bachellier P, Nuzzo G, Belghiti J, Pruvot FR and Regimbeau JM: AJCC 7th edition of TNM staging accurately discriminates outcomes of patients with resectable intrahepatic cholangiocarcinoma. Cancer 117: 2170-2177, 2011.
14. Livak KJ and Schmittgen TD: Analysis of relative gene expression data using real-time quantitative PCR and the 2(-Delta Delta C (T)) method. Methods 25: 402-408, 2001.
15. Renshaw S: Immunohistochemistry and immunocytochemistry: Essential methods. John Wiley Sons 6: 248, 2017.
16. Li J, Guan HY, Gong LY, Song LB, Zhang N, Wu J, Yuan J, Zheng YJ, Huang ZS and Li M: Clinical significance of sphingosine kinase-1 expression in human astrocytomas progression and overall patient survival. Clin Cancer Res 14: 6996-7003, 2008.
17. Koya Y, Kajiyama H, Liu W, Shibata K, Senga T and Kikkawa F: Murine experimental model of original tumor development and peritoneal metastasis via orthotopic inoculation with ovarian carcinoma cells. J Vis Exp 9: 54353, 2016.
18. Shu YJ, Weng H, Ye YY, Hu YP, Bao RF, Cao Y, Wang XA, Zhang F, Xiang SS, Li HF, *et al*: SPOCK1 as a potential cancer prognostic marker promotes the proliferation and metastasis of gallbladder cancer cells by activating the PI3K/AKT pathway. Mol Cancer 14: 12, 2015.

19. Tian F, Xu F, Zhang ZY, Ge JP, Wei ZF, Xu XF and Cheng W: Expression of CHD1L in bladder cancer and its influence on prognosis and survival. Tumor Biol 34: 3687-3690, 2013.
20. Ji X, Li J, Zhu L, Cai J, Zhang J, Qu Y, Zhang H, Liu B, Zhao R and Zhu Z: CHD1L promotes tumor progression and predicts survival in colorectal carcinoma. J Surg Res 185: 84-91, 2013.
21. Zhong D, He G, Zhao S, Li J, Lang Y, Ye W, Li Y, Jiang C and Li X: LRG1 modulates invasion and migration of glioma cell lines through TGF-β signaling pathway. Acta Histochem 117: 551-558, 2015.
22. Xu X, He Y, Miao X, Wu Y, Han J, Wang Q, Liu J, Zhong F, Ou Y, Wang Y and He S: Cell adhesion induces overexpression of chromodomain helicase/ATPase DNA binding protein 1-like gene (CHD1L) and contributes to cell adhesion-mediated drug resistance (CAM-DR) in multiple myeloma cells. Leuk Res 47: 54-62, 2016.
23. He LR, Ma NF, Chen JW, Li BK, Guan XY, Liu MZ and Xie D: Overexpression of CHD1L is positively associated with metastasis of lung adenocarcinoma and predicts patients poor survival. Oncotarget 6: 31181-31190, 2015.
24. Liu C, Fu X, Zhong Z, Zhang J, Mou H, Wu Q, Sheng T, Huang B and Zou Y: CHD1L expression increases tumor progression and acts as a predictive biomarker for poor prognosis in pancreatic cancer. Dig Dis Sci 62: 2376-2385, 2017.
25. He Q, Cai L, Shuai L, Li D, Wang C, Liu Y, Li X, Li Z and Wang S: Ars2 is overexpressed in human cholangiocarcinomas and its depletion increases PTEN and PDCD4 by decreasing microRNA-21. Mol Carcinog 52: 286-296, 2013.
26. Yang XQ, Xu YF, Guo S, Liu Y, Ning SL, Lu XF, Yang H and Chen YX: Clinical significance of nerve growth factor and tropomyosin-receptor-kinase signaling pathway in intrahepatic cholangiocarcinoma. World J Gastroenterol 20: 4076-4084, 2014.
27. Shen G, Lin Y, Yang X, Zhang J, Xu Z and Jia H: MicroRNA-26b inhibits epithelial-mesenchymal transition in hepatocellular carcinoma by targeting USP9X. BMC Cancer 14: 393, 2014.
28. Green DR and Chipuk JE: p53 and metabolism: Inside the TIGAR. Cell 126: 30-32, 2006.
29. Zolota V, Sirinian C, Melachrinou M, Symeonidis A and Bonikos DS: Expression of the regulatory cell cycle proteins p21, p27, p14, p16, p53, mdm2, and cyclin E in bone marrow biopsies with acute myeloid leukemia. Correlation with patients' survival. Pathol Res Pract 203: 199-207, 2007.
30. Chen M, Huang JD, Hu L, Zheng BJ, Chen L, Tsang SL and Guan XY: Transgenic CHD1L expression in mouse induces spontaneous tumors. PLoS One 4: e6727,2009.
31. López-Soto A, Gonzalez S, Smyth MJ and Galluzzi L: Control of metastasis by NK cells. Cancer Cell 32: 135-154, 2017.
32. Zhou W, Ye XL, Xu J, Cao MG, Fang ZY, Li LY, Guan GH, Liu Q, Qian YH and Xie D: The lncRNA H19 mediates breast cancer cell plasticity during EMT and MET plasticity by differentially sponging miR-200b/c and let-7b. Sci Signal 10: eaak9557, 2017.
33. Kang Y and Massagué J: Epithelial-mesenchymal transitions: twist in development and metastasis. Cell 118: 277-279, 2004.
34. Chen L, Chan TH, Yuan YF, Hu L, Huang J, Ma S, Wang J, Dong SS, Tang KH, Xie D, *et al*: CHD1L promotes hepatocellular carcinoma progression and metastasis in mice and is associated with these processes in human patients. J Clin Invest 120: 1178-1191, 2010.